AJNR

The suboccipital carrefour: cervical and vertebral arterial anastomosis.

M Ayad, F Viñuela and E H Rubinstein

AJNR Am J Neuroradiol 1998, 19 (5) 925-931
http://www.ajnr.org/content/19/5/925

AJNR Am J Neuroradiol 19:925–931, May 1998

The Suboccipital Carrefour: Cervical and Vertebral Arterial Anastomosis

Michael Ayad, Fernando Viñuela, and Eduardo H. Rubinstein

PURPOSE: **Our objective was to anatomically define the anastomoses between cervical and carotid arterial distributions (the carrefour) in the rabbit and to assess the contribution of these collaterals to cortical blood flow (CBF) during cerebral ischemia.**

METHODS: **Angiography was carried out in six rabbits with basilar artery occlusion using selective contrast injection into the right subclavian, external carotid, and internal carotid arteries. Anastomoses were corroborated with methacrylate vascular casts prepared in five additional rabbits. CBF was measured in eight rabbits by H_2 clearance after basilar artery occlusion and again after bilateral common carotid artery occlusion. Cortical DC potential was measured during ischemia in these rabbits and in another 19 rabbits after additional occlusion of the cervical collateral arteries.**

RESULTS: **A network of anastomoses between superficial and ascending cervical, superior intercostal, vertebral, and occipital arteries was found by angiography and corrosion casts. Additional communications in the ophthalmic, ethmoidal, and cerebellar arterial distributions are described. These pathways were found to supply a mean of 15 ± 7 mL/100 g per minute residual CBF during three-vessel ischemia, or 24% of the preischemic CBF. Ischemic depolarization of DC potential occurred in seven of the eight rabbits with collateral CBF at a mean latency of 2.64 ± 0.59 minutes and at 1.71 ± 0.09 minutes in those without.**

CONCLUSION: **The suboccipital collateral network of the rabbit resembles that of humans and can contribute significantly to CBF during ischemia. The results suggest that this model may be useful for evaluating methods of optimizing hemodynamic control of the anastomoses in situations such as those encountered during endovascular therapy.**

The suboccipital carrefour or "knot" refers to a network of anastomoses interconnecting the cervical, vertebral, occipital, and carotid arteries that has been well described in humans (1). The functional significance of this arterial network stems from its recruitment during pathologic conditions of arterial occlusion or in the presence of local vascular malformations. After stenosis of the common carotid artery, the suboccipital carrefour enlarges to provide collateral blood flow from subclavian to external carotid territories, ultimately supplying the brain by way of intraorbital ophthalmic anastomoses (2, 3). A reversed pattern of flow in the system occurs after proximal subclavian artery occlusion, contributing to the so-called subclavian steal phenomenon (4, 5). The extent and directionality of flow through the anastomoses are clearly dependent on the pressure gradient across the channels (6), thus explaining the variability of their opacification on routine angiography (7).

The present study was undertaken to characterize the arterial network described above in the rabbit. This animal possesses a well-developed circle of Willis and brain blood flow, which, like that of humans, is not confounded by the presence of a rete mirabile. A protocol involving proximal basilar artery occlusion and selective injection of the subclavian artery with contrast material was used to optimize the pressure gradient and thus to visualize the collateral system during angiography. To correlate the angiographic results with three-dimensional anatomy, methacrylate arterial casts were prepared of the craniocervical vasculature. Second, the potential contribution of the suboccipital collateral system to brain blood flow during ischemia was measured by using the hydrogen clearance method (8). Finally, a functional correlate of this collateral blood flow was determined by measuring the latency for the onset of ischemic depolarization of cortical DC potential. This index was recorded in rabbits with basilar and bilateral carotid artery occlusion alone (and thus preserved suboccip-

Received August 29, 1997; accepted October 12.

From the Departments of Anesthesiology (E.H.R.), Physiology (M.A., E.H.R.), and Radiological Sciences (F.V.), UCLA School of Medicine, Los Angeles.

Address reprint requests to Eduardo H. Rubinstein, MD, PhD, Department of Anesthesiology, UCLA School of Medicine, Los Angeles, CA 90024.

ital collateral blood flow) as compared with that in rabbits with additional blockade of the collateral blood flow.

Methods

Experiments were carried out on male New Zealand white rabbits weighing between 2.8 and 4.0 kg. The protocols were approved by the Chancellor's Animal Research Committee and were in compliance with NIH guidelines for the care and use of laboratory animals. All rabbits underwent induction of anesthesia with 5% halothane in an enclosed chamber followed by tracheotomy, intubation, and mechanical ventilation. Paralysis was maintained with intravenous pancuronium bromide (0.3 mg/kg per hour). Halothane was then reduced to 0.8% for the duration of the experiment and respiratory rate was adjusted to maintain an end-tidal P_{CO_2} of 26 mm Hg. Esophageal temperature was maintained at 38.0°C with radiant heat throughout the experiment. The femoral artery and vein were catheterized for measurement of arterial blood pressure and fluid or drug administration, respectively.

Angiography

To isolate the vertebral arteries from the circle of Willis, we approached the proximal basilar artery via retropharyngeal craniotomy and occluded it with bipolar electrocautery for a distance of 2 mm beginning at the vertebrobasilar junction. Both internal and external carotid arteries were carefully exposed at their bifurcation, and 4-0 silk ligatures were placed loosely around the two arteries on the right for selective occlusion with an aneurysmal clip during angiography. On the left side, the external carotid artery was ligated at its origin to prevent reflux of contrast material from that artery into the brain circulation. At the midpoint between the carotid bifurcation and aorta, the right common carotid artery was cannulated with two 5F catheters, each extending for 1.5 cm in either direction. The rostrally directed catheter was used for injecting contrast material into the occipital, internal, and external carotid arteries. The aortic arch was then exposed through a sternotomy at the second intercostal space. Nylon snares were placed around the left subclavian artery and brachicephalic trunk, sparing the left common carotid artery. Occlusion of the brachiocephalic trunk permitted selective perfusion of the right subclavian artery when contrast material was injected into the caudally directed right carotid catheter. The left subclavian artery was occluded during angiography to induce a subclavian steal and thus to increase retrograde filling of the cervical collateral vessels on that side with contrast agent. Similarly, the left common carotid artery was transiently occluded with a bulldog during angiography to induce cerebral ischemia and to improve the pressure gradient for anterograde filling of anastomotic vessels to the brain circulation.

Six rabbits underwent angiography. In each rabbit, angiograms were taken during separate injections of contrast material into the right external carotid, right internal carotid, and right subclavian arteries; each injection was replicated at least once. Anastomotic arteries between the subclavian, external, and internal carotid territories were readily identifiable by their presence on arteriograms taken from selective injection of two different arteries; the larger anastomoses were often visible on each of the three different series. All arteriograms were taken in the supine position using Omnipaque contrast medium. The amount of contrast agent used varied with the artery injected approximately as follows: external carotid artery, 4 mL; internal carotid artery, 2.5 mL; subclavian artery, 6 mL. Digitally subtracted arteriograms were taken in an angiography room using a GE AdvantX system at a frame rate of 7.5 per second.

Vascular Cast Preparation

Anatomic casts of the cervical and cerebral vasculature were prepared in five rabbits. The abdominal aorta was catheterized in two animals with a plastic cannula directed toward the heart (inner diameter, 3.5 mm; outer diameter, 4.9 mm). In one of these rabbits, the basilar artery and both common carotid arteries were occluded before injection of contrast material. The remaining two rabbits first underwent occlusion of the basilar artery and both common carotid arteries followed by placement of a centrally directed 5F catheter in the right carotid and a snare around the brachiocephalic trunk. The internal carotid arteries were occluded bilaterally in one of the two rabbits. Filling of the suboccipital collateral network was achieved by central injection into the carotid catheter following snare occlusion of the brachiocephalic trunk.

After completion of the vessel preparations described above, each rabbit was killed with an intravenous injection of 3 mEq KCl. The craniocervical vasculature was then perfused with 60 to 120 mL of normal saline containing 10 U/mL heparin and 50 μg/mL papaverine until the effluent from an opened external jugular vein was clear. Methyl methacrylate monomer, catalyst, coloring agent, and promoter were prepared in a ratio of 200:30:12:1 (Batson's #17 Anatomical Corrosion Compound, Polysciences, Warrington, Pa), and approximately 30 mL was injected under hand pressure into either the aortic or carotid catheter. The thorax was then hemisected and the upper body immersed in cold water for 3 hours to facilitate curing of the acrylic resin. After the polymerization was complete, the specimens were placed in 35% KOH to dissolve soft tissues and bone.

Measurement of Collateral Blood Flow and DC Potential

In eight rabbits, nylon snares were placed around both common carotid arteries following basilar artery occlusion, and the animals were placed prone in a stereotactic head frame. Bilateral parietal craniotomies 5 mm in diameter were made just caudal to the coronal suture and lateral to the midline. The dura mater of the left hemisphere was pierced and a Teflon-coated platinum-iridium (Pt-Ir) wire electrode (0.005-inch diameter bare; 0.007-inch diameter coated) was advanced 1 mm into the cerebral cortex using a Narishige (Stoelting; Wood Dale, IL) micromanipulator. Current between the Pt-Ir electrode and an indifferent silver-silver chloride (Ag-AgCl) electrode placed on the lumbar trapezius muscle was measured with a polarographic amplifier polarized to +400 mV. For determination of cortical blood flow (CBF), hydrogen was added to the inspired gas mixture ($FI_{H_2} = 0.1$) and maintained until the hydrogen current reached a stable plateau for at least 2 minutes, signifying saturation of cerebral tissue with H_2. Inflow of H_2 was then stopped and the desaturation slope recorded. In each animal, CBF was first measured under baseline conditions; that is, basilar artery occlusion alone. Blood flow was then remeasured during bilateral carotid occlusion. In the calculation of CBF, the first 1.5 minutes of each desaturation was deleted in order to avoid recirculation artifacts. The remaining data were normalized, plotted, and fitted by computer with an exponential equation. The half-time for washout in minutes ($t_{1/2}$) was derived from the exponential equation, and CBF was then calculated according to the expression $CBF = (100) \ln(2/t_{1/2})$, giving values in mL/100 g per minute (8).

To measure cortical DC potential, a second Ag-AgCl electrode mounted within a glass pipette containing Ringer's solution was placed on the pial surface of the right parietal cortex via a cotton bridge. The potential difference between the active and indifferent electrodes was recorded on a Neuroprobe DC amplifier (A-M Systems; Everett, WA) with input impedance of 10^{11} ohms. DC potential was also recorded in 19 rabbits that, in addition to undergoing occlusion of the basilar and bilateral carotid arteries, underwent ligation of the subclavian vessels that supply inflow to the suboccipital collateral network. In these animals, the proximal subclavian, vertebral, internal thoracic, superior intercostal, and superficial cervical arteries were ligated bilaterally before the induction of cerebral ischemia by

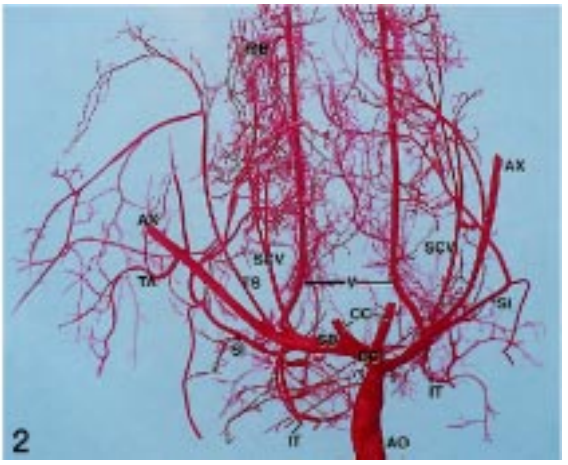

FIG 1. Angiogram of the right subclavian artery vasculature in the rabbit. Contrast material was injected in the right common carotid artery during proximal occlusion of the brachiocephalic trunk. (Definitions for abbreviations used in all figures are in box.)

FIG 2. Methacrylate corrosion cast of the proximal aortic arch obtained by retrograde perfusion of the right common carotid artery with resin. Note the ascending branch of the superior intercostal artery, which anastomoses with fine branches of the superficial cervical and muscular branches of the vertebral arteries.

snare occlusion of the brachiocephalic trunk. The latter set of experiments was carried out as part of a separate in-depth electrophysiological study.

Statistical Analysis

The results of CBF and latency of DC potential onset are expressed as mean ± SEM. Comparisons of DC onset between animals with collateral CBF and those without were carried out using factorial analysis of variance and Scheffe's test for multiple comparisons. *P* values less than .05 were considered statistically significant.

Results

Figure 1 is an angiogram depicting the primary branches of the subclavian artery in the rabbit. A typical pattern seen in a corrosion cast specimen of the aortic arch is shown in Figure 2 for comparison. The vertebral artery, the most proximal branch of the subclavian artery, courses dorsomedially through the transverse foramena of the first six cervical vertebrae, giving off muscular branches at each intervertebral level. The superficial cervical artery arises anterior to the vertebral origin. Traveling in the ventrolateral neck, it often gives off an ascending cervical branch, as seen in Figure 1. Both the superficial and ascending cervical arteries fuse at various points with muscular branches of the vertebral artery. The superior intercostal artery and the internal thoracic artery usually arise from a common trunk on the inferior aspect of the subclavian just distal to the vertebral origin. The internal thoracic artery descends along the ventral thoracic wall anastomosing with intercostal arteries arising from the descending aorta. The intercostal arteries are not seen in Figure 1 because of an unfavorable pressure gradient during contrast injection, because they were under pressure from the aorta. However, the internal thoracic-intercostal anastomoses down to the T7–8 costal level were present on both vascular casts obtained by perfusion of the abdominal aorta. The superior intercostal artery (sometimes referred to as the costocervical artery) bifurcates the descending artery, giving off branches that supply the lateral aspect of the first three ribs. The ascending superior intercostal branch courses as high as the C-3 vertebral level, ramifying extensively with

Key to Abbreviations of Arteries

AA	anterior auricular
AC	anterior cerebral
ACV	ascending cervical
AIC	anterior inferior cerebellar
AO	aorta
AP	ascending pharyngeal
AS	anterior spinal
AX	axillary
B	basilar
BC	brachiocephalic
CA*	cerebellar anastomoses
CC	common carotid
CL	ciliary
DBOC	descending branch of occipital
EC	external carotid
EE	external ethmoidal
ET*	ethmoidal rete
EO	external ophthalmic
F	facial
FR	frontal
IC	internal carotid
IM	internal maxillary
IO	internal ophthalmic
IT	internal thoracic
L	lingual
LT	lateral thoracic
MB	muscular branches of vertebral
MC	middle cerebral
OC	occipital
OP*	ophthalmic anastomosis
PA	posterior auricular
PB	perforating branches of basilar
PC	posterior cerebral
PIC	posterior inferior cerebellar
SB	subclavian
SC	superior cerebellar
SCV	superficial cervical
SI	superior intercostal
SS	subscapular
ST	superficial temporal
TA	thoracoacromial
TF	transverse facial
TS	transverse scapular
V	vertebral
VOC*	vertebral-occipital anastomosis

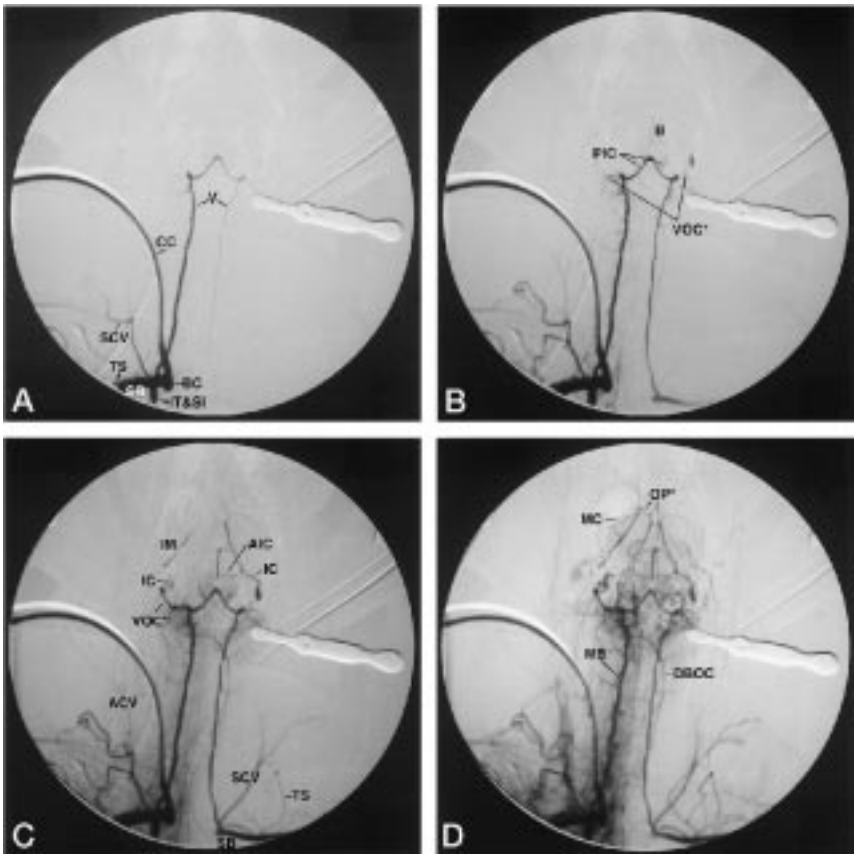

FIG 3. Serial frames of an angiogram taken by the same methods as Figure 1 show filling of the cerebral vasculature solely by collateral input. The proximal basilar artery and both external carotid arteries have been occluded.

A, Taken 1.72 seconds after the beginning of contrast injection.

B, At 2.13 seconds, note filling of the basilar artery via cerebellar collaterals.

C, At 3.19 seconds, large vertebral-occipital anastomoses permit filling of the circle of Willis by way of the common origins of the internal carotid and occipital arteries.

D, At 7.06 seconds, note the ophthalmic anastomoses between the internal and external carotid arterial territories. The extensive course of descending branches of the occipital artery is also evident.

branches of the superficial cervical artery as well as with muscular branches of the vertebral artery, as shown in Figure 2. The transverse scapular artery has wide variability in its site of origin from the subclavian, but in this series of experiments it was found to arise most frequently several millimeters distal to the superficial cervical artery on the superior aspect of the subclavian artery. In two instances, the superficial cervical artery was found to arise from a proximally located transverse scapular artery. The transverse scapular artery itself passes over the scapula and was not found to anastomose appreciably with the superior intercostal, superficial cervical, or vertebral arteries.

The serial angiograms in Figure 3 illustrate the function of the cervical vasculature as a collateral pathway to the cerebral circulation. Direct inflow to the circle of Willis was blocked by prior occlusion of the proximal basilar artery and both common carotid arteries. Selective perfusion of the right subclavian artery in Figure 3A shows early filling of its primary branches, including a common origin of the superficial cervical and transverse scapular arteries and retrograde filling of the contralateral vertebral artery. In Figure 3B, 0.41 seconds later, even though its origin is occluded, the basilar artery begins to fill via anastomoses between the posterior and anterior cerebellar arteries arising from the vertebral and basilar arteries, respectively. Muscular branches of the vertebral artery are also apparent, the largest of which, at the C-1 level, becomes the prominent anastomosis between the vertebral and occipital arteries. In this particular rabbit, the diameter of the vertebral-occipital anastomosis approximates the caliber of the vertebral artery itself. Because of the common origins of the occipital and internal carotid arteries in this rabbit, later images (Fig 3C and D) show anterograde filling of the circle of Willis via the internal carotid artery. In addition, a contribution to the circle of Willis from the external carotid distribution can be appreciated. The ophthalmic anastomosis between the ciliary branch of the internal maxillary artery and the internal ophthalmic branch of the internal carotid artery is clearly visible in Figure 3D.

In contrast to Figure 3, the occipital artery may arise from a variety of different origins in the rabbit. Figure 4 shows the occipital artery originating near the trifurcation of the external carotid artery, where it forms an anastomotic ring with the superficial temporal artery and gives off numerous descending branches. While the vertebral occipital anastomosis constitutes the principal collateral pathway from the cervical vasculature to the carotid territory, the extensive ramifications of the descending branch of the occipital artery communicate with other cervical vessels as well. This can best be seen in the vascular cast shown in Figure 5. A large vertebral-occipital anastomosis is present in this specimen. The tortuous occipital artery and its descending branches form an anastomotic plexus with the ascending cervical artery and, to a lesser extent, with the superficial cervical artery from which the ascending cervical artery arises. Muscular branches of the vertebral artery contribute to

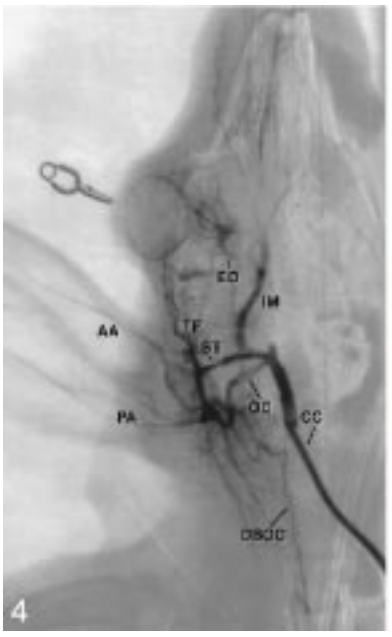

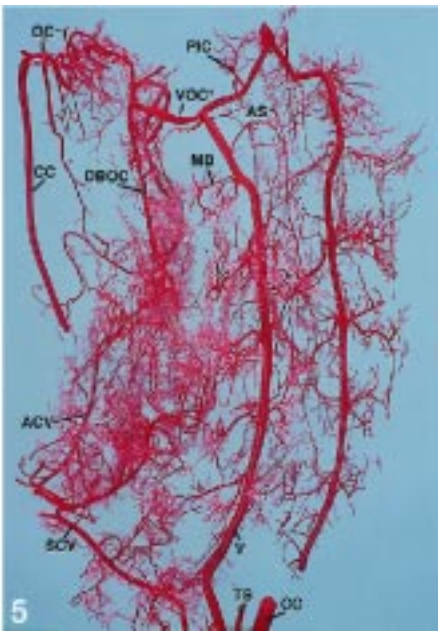

FIG 4. Selective injection of contrast material into the occipital and internal maxillary arteries (facial, lingual, and internal carotid arteries have been ligated). Note the distal origin of the occipital artery (as compared with Fig 3) and the anastomotic ring formed between the occipital and superficial temporal arteries.

FIG 5. Anterior oblique view. Corrosion cast of the suboccipital carrefour prepared by perfusion of the right subclavian artery with resin (internal and external carotid arteries have been ligated). The right common carotid artery has been rotated laterally to provide exposure of the extensive anastomotic network between the anterior and superficial cervical arteries, the muscular branches of the vertebral artery, and the descending branches of the occipital artery. The anterior spinal artery, terminating in the distal vertebral arteries, is also apparent in this specimen.

the carrefour at multiple levels as well. Although not shown in this cast, the ascending branch of the superior intercostal artery contributes to a variable extent from one rabbit to another.

The anastomoses between the internal and external carotid arteries, which permit suboccipital collateral inflow to or outflow from the brain (depending on the pressure gradient), are shown in Figures 6 and 7. Figure 6 shows angiographic filling of the internal maxillary arteries after selective injection of contrast material into the right internal carotid artery. The internal ophthalmic artery, taking origin from the internal carotid artery shortly before joining the circle of Willis, travels for a short distance and branches to give off two to three parallel vessels that supply the retina and sclera. The more distal vessel of the group then bifurcates at almost 180°. The medial arm of this bifurcation fuses in the midline with its contralateral counterpart and gives off small branches that join the ethmoidal arteries anteriorly. The lateral branch of this internal ophthalmic artery joins the ciliary artery, arising from the external ophthalmic branch of the internal maxillary artery, to make up the ophthalmic anastomosis. As seen in Figure 7, the short external ophthalmic artery also gives off the frontal artery, which travels rostromedially. The frontal artery gives rise to one or more external ethmoidal arteries, which meet in the midline with the contralateral external ethmoidal vessel(s). The anterior cerebral arteries fuse in the midline to form a common trunk that travels a short distance before anastomosing with the ethmoidal arteries and midline branch of the internal ophthalmic artery to make up the ethmoidal rete.

Two other sources of collateral blood flow may be

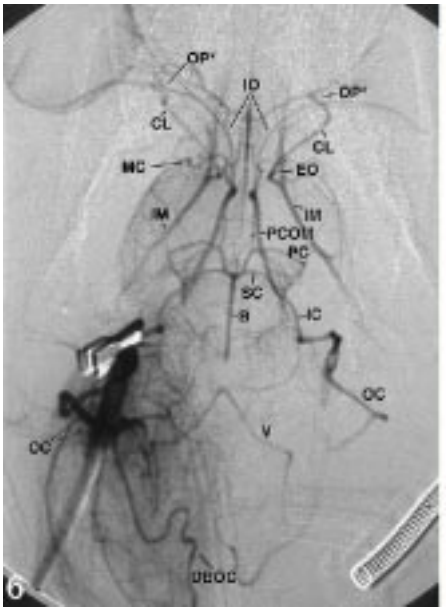

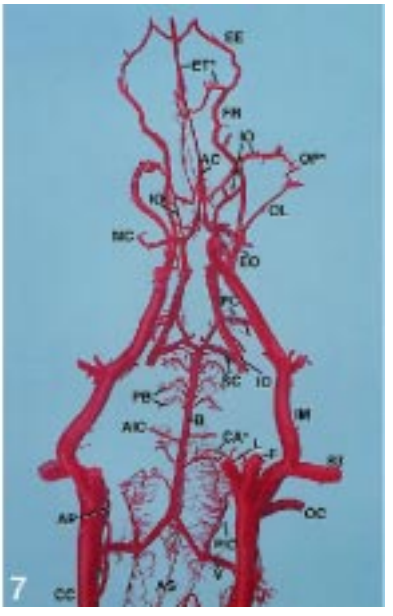

FIG 6. Selective injection of contrast material into the right internal carotid artery. The ophthalmic anastomosis between the ciliary branch of the external and internal ophthalmic arteries is clearly displayed.

FIG 7. Dorsal view of the corrosion cast of the internal maxillary arteries and circle of Willis displays the ophthalmic anastomoses, ethmoidal rete, and cerebellar collateral circle (descriptions are in text).

appreciated from Figure 7. The cerebellar collateral circle, between the anterior and posterior inferior cerebellar arteries, is apparent in this cast, which may allow blood or contrast material to bypass the vertebrobasilar junction, as in the angiograms in Figure 3. The anterior spinal artery, seen in Figures 5 and 7, provides a potential small accessory pathway from the aorta to the vertebral artery, since it also receives radicular input from the posterior intercostal and lumbar arteries. Small communications between descending thyroid arterial branches of the common carotid artery and tracheal branches derived from the superior intercostal artery were also found in two of the corrosion casts, but were not seen angiographically.

Cortical blood flow measured by the H_2 clearance method in eight rabbits with occlusion of the basilar artery alone was 62.2 ± 6.9 mL/100 g per minute. Repeat measurements taken after occlusion of bilateral common carotid arteries gave a mean CBF of 15.0 ± 7.0 mL/100 g per minute, or 24% of the baseline flow. This residual flow represents collateral CBF that can be accounted for by the pathways discussed in the previous section.

The latency for ischemic depolarization of DC potential was measured in eight rabbits during bilateral common carotid artery occlusion after prior cautery of the basilar artery alone. Ischemic depolarization occurred in seven of the eight rabbits; the mean latency of ischemic depolarization was 2.64 ± 0.59 minutes. The rabbit that did not elicit ischemic depolarization had a baseline CBF of 74.4 mL and ischemic CBF of 58.5 mL/100 g per minute. The completeness of the occlusions in this animal were verified and ischemia was replicated, giving comparable CBF results. Therefore, this unusually high residual CBF value was not attributable to inadvertent patency of the common carotid arteries or vertebrobasilar junction. If the CBF values in this rabbit were excluded from the overall analysis, the mean baseline and ischemic CBF of the remaining animals were 61.0 and 8.8 mL/100 g per minute, respectively. Ischemia without residual flow was produced in 19 rabbits with prior bilateral occlusion of the vertebral, superficial cervical, superior intercostal, and internal thoracic arteries. All of these animals exhibited ischemic depolarization, with a mean latency of 1.71 ± 0.09 minutes. The difference in ischemic depolarization latency between the seven rabbits with residual flow compared with those without it was statistically significant at $P = .03$.

Discussion

Whereas the suboccipital collateral system has been extensively described in humans (1–4, 9–12), its presence in experimental animals has not been nearly so well appreciated. This study has found a surprising degree of similarity between the cervical collateral network of the rabbit and that of humans, suggesting that the rabbit may be a useful model for further studies of the carrefour's physiological function in various occlusive states.

By and large, our findings correspond to the basic anatomy that has previously been identified in the rabbit; however, the literature contains some discrepancies. Bensley (13) described the transversa colli artery as arising from the subclavian artery and coursing toward the neck of the first rib. This depiction was not documented by other authors (14, 15), and in the specimens reported here, the artery was a branch of the superior intercostal artery, which did not contribute to the cervical collateral plexus. Similarly, the thyroidea ima artery, arising from the brachiocephalic trunk to supply the trachea and infrahyoid musculature, has been inconsistently observed by different authors (13–16) and was not found in the corrosion casts studied here. The ascending pharyngeal artery is a small vessel sometimes present in the rabbit. Arising medially from the carotid bifurcation, it has been observed by some authors (17, 18) but not by others (19–21). The ascending pharyngeal artery was identified in two vascular cast specimens in the present study (eg, Fig 7), but in neither case did the artery anastomose with the occipital artery, as it often does in humans (1, 12).

While the collective cervical collateral pathway reported here has not previously been examined in the rabbit, some of the individual anastomoses have been described. The vertebral-occipital anastomosis was briefly mentioned in two accounts (17, 20) but refuted by Jeppsson and Olin (18). Their failure to observe the communication angiographically was most likely due to the absence of a pressure gradient during contrast injection in their preparation, as is often the case in humans (6). Wide variability in the origin of the occipital artery of the rabbit has been reported by several authors (18, 19, 21). The anastomoses between superficial temporal and occipital arteries and between descending branches of the occipital artery and ascending and superficial cervical arteries have not, to our knowledge, been previously described. Ophthalmic (17–20) and ethmoidal (19, 20) anastomoses between the internal and external carotid circulations in the rabbit have previously been documented in varying degrees of detail. The collateral circle between the anterior and posterior inferior cerebellar arteries and perforating branches of the basilar artery found here was also present in the corrosion casts of Freisenhausen (22).

The anatomic, CBF, and DC potential data all suggest that the suboccipital collateral system may exhibit significant variability from one rabbit to the next. On the other hand, its contribution to CBF under ischemic conditions does not appear to be trivial, and, in fact, in some animals it was considerable. Overall it represented 24% of the preischemic CBF values in this series. The preischemic flow of 62 mL/100 g per minute obtained with basilar occlusion alone is within the normal range of CBF for this species (19). An unknown but probably small component of the residual CBF may be attributed to flow in the cerebellar collateral anastomoses (Figs 3A and 7) across the vertebrobasilar junction. Another small potential source of inflow into the suboccipital plexus may have come from anterograde flow from the an-

terior spinal artery into the vertebral artery supplied by thoracolumbar radicular arteries.

Apart from the animal with aberrantly high residual CBF, the collateral flow in the remaining seven rabbits was below the threshold for ischemic depolarization of DC potential. However, the latency was significantly prolonged relative to rabbits without collateral blood flow. This delay in ischemic depolarization suggests that the collateral flow may be of sufficient volume to alter the outcome from a transient ischemic episode (23, 24). Moreover, this blood flow represents the capacity of preexisting collaterals during an acute event, before there is time for adaptation. Symon and Russell (25) found that primates could tolerate bilateral occlusion of both the vertebral and carotid arteries without apparent brain damage provided that the ligations were carried out sequentially over several months. They concluded that the progressive enlargement of cervical collateral anastomoses accounted for this remarkable tolerance.

The clinical significance of the suboccipital carrefour in endovascular therapy has been recognized by neuroradiologists both for its potential benefits and for its hazards. During embolization of arteriovenous malformations supplied by occipital or cervical arteries, there is a potential risk of an embolic agent escaping into the cerebral circulation via the craniocervical anastomoses. Several reports have described this complication (26–28). Direction of flow in the carrefour during this procedure is thought to depend on many factors, including rate and force of injection, local tissue ischemia caused by obliteration of feeding vessels, P_{CO_2}, and systemic arterial pressure (26, 29). Another situation in which the cervical collateral system may be problematic is after external or common carotid artery ligation to control operative bleeding during head and neck surgery (30). In some cases, ligation of the occipital or cervical arteries has been necessary to adequately reduce bleeding. These situations underscore the importance of understanding the variables influencing hemodynamics of this arterial system in various circumstances.

Conclusion

A network of anastomoses between ascending cervical, superficial cervical, superior intercostal, vertebral, and occipital arteries has been described in the rabbit by means of angiography and methacrylate vascular casts. Measurements of blood flow and DC potential indicate that the contribution of this network to CBF during ischemia may be variable but significant. The results suggest that the arterial system of the rabbit may be a useful model by which to study the hemodynamics of collateral blood flow to the brain. Of particular interest would be the hemodynamic response of the collaterals to pharmacologic manipulation, chronic ischemia, P_{CO_2}, and hypertension.

Acknowledgments

We thank John Roberts and Christopher Carungi for their technical assistance during angiography.

References

1. Lasjaunias P, Berenstein A. *Surgical Neuroangiography, 1: Functional Anatomy of Craniofacial Arteries.* New York: Springer; 1987:283–292
2. Miyachi S, Negoro M, Sugita K. **The occipital-vertebral anastomosis as a collateral pathway: hemodynamic patterns.** *Surg Neurol* 1989;32:350–355
3. Zülch KJ. **Some basic patterns of the collateral circulation of the cerebral arteries.** In: Zülch KJ, ed. *Cerebral Circulation and Stroke.* New York: Springer; 1971:1106–1122
4. Bosniak MA. **Cervical arterial pathways associated brachiocephalic occlusive disease.** *AJR Am J Roentgenol* 1964;91:1232–1244
5. Herring M. **The subclavian steal syndrome: a review.** *Am Surg* 1977;43:220–228
6. Mosmans PCM, Jonkman EJ. **The significance of the collateral vascular system of the brain in shunt and steal syndromes.** *Clin Neurol Neurosurg* 1980;82:145–156
7. Seeger JF, Gabrielson TO, Latchaw RE. **Some technique-dependent patterns of collateral flow during cerebral angiography.** *Neuroradiology* 1974;8:149–155
8. Young W. **H_2 clearance measurement of blood flow: a review of technique and polarographic principles.** *Stroke* 1980;11:552–564
9. Fields WS, Bruetman ME, Weibel J. **Collateral circulation of the brain.** *Mongraph Surg Sci* 1965;2:183–259
10. Peeters FLM. **Collateral circulation between the external and internal carotid arteries.** *Diagn Imaging Clin Med* 1981;50:91–98
11. Schechter MM. **The occipital-vertebral anastomosis.** *J Neurosurg* 1964;21:758–762
12. Pelz DM, Fox AJ, Vinuela F, et al. **The ascending pharyngeal artery: a collateral pathway in complete occlusion of the internal carotid artery.** *AJNR Am J Neuroradiol* 1987;8:177–178
13. Bensley BA. *Practical Anatomy of the Rabbit.* 3rd ed. Philadelphia: Blakiston; 1921
14. Baldwin FM. **Notes on the branches of the aorta (arcus aortae) and the subclavian artery of the rabbit.** *Anat Rec* 1920;19:173–183
15. Angell-James JE. **Variations in the vasculature of the aortic arch and its major branches in the rabbit.** *Acta Anat* 1974;87:283–300
16. Bugge J. **Arterial supply of the cervical viscera in the rabbit.** *Acta Anat* 1967;68:216–227
17. Daniel PM, Dawes JDK, Pritchard MML. **Studies of the carotid rete and its associated arteries.** *Phil Trans R Soc London (Series B)* 1953;237:173–215
18. Jeppsson PG, Olin T. **Cerebral angiography in the rabbit: an investigation of vascular anatomy and variations in circulatory pattern with conditions of injection.** *Lund Univ Arsskkr N F Avd* 1960;56:1–56
19. Scremin OU, Sonnenschein RR, Rubinstein EH. **Cerebrovascular anatomy and blood flow measurements in the rabbit.** *J Cereb Blood Flow Metab* 1982;2:55–66
20. Chungcharoen D, DeBurgh Daly M, Neil E, Schweitzer A. **The effect of carotid occlusion upon the intrasinusal pressure with reference to vascular communications between the carotid and vertebral circulations in the dog, cat and rabbit.** *J Physiol* 1952;117:56–76
21. Baldwin FM. **Variations in the carotid arteries of the rabbit.** *Anat Rec* 1919;16:309–315
22. Freisenhausen H-D. **Gefassanordnung und Kapillardichte im Gehirn des Kaninchens.** *Acta Anat* 1965;62:539–562
23. Astrup J, Siesjo BK, Symon L. **Thresholds in cerebral ischemia: the ischemic penumbra.** *Stroke* 1981;12:723–725
24. Ayad M, Verity MA, Rubinstein EH. **Lidocaine delays cortical ischemic depolarization: relationship to electrophysiologic recovery and neuropathology.** *J Neurosurg Anesthesiol* 1994;6:98–110
25. Symon L, Russell RWR. **The development of cerebral collateral circulation following occlusion of vessels in the neck: an experimental study in baboons.** *J Neurol Sci* 1971;13:197–208
26. Spetzler RF, Modic M, Bonstelle C. **Spontaneous opening of large occipital-vertebral artery anastomosis during embolization.** *J Neurosurg* 1980;3:849–850
27. Ahn HS, Kerber CW, Deeb ZL. **Extra- to intracranial arterial anastomoses in therapeutic embolization: recognition and role.** *AJNR Am J Neuroradiol* 1980;1:71–75
28. Bitoh S, Hasegawa H, Obashi J, Maruno M. **Sudden appearance of occipital-vertebral arterial anastomoses during therapeutic embolization.** *Surg Neurol* 1985;24:160–164
29. Russell EJ. **Functional angiography of the head and neck.** *AJNR Am J Neuroradiol* 1986;7:927–936
30. Takeuchi Y, Numata T, Konno A, Suzuki H, Hino T, Kaneko T. **Hemodynamic changes in the head and neck after ligation of the unilateral carotid arteries: a study using color Doppler imaging.** *Ann Otol Rhinol Laryngol* 1994;103:41–45